Available online at www.sciencedirect.com
ScienceDirect
Physica B 399 (2007) 138–142
PHYSICA B
www.elsevier.com/locate/physb

Examining crystallographic orientation dependence of hardness of silica stishovite

Sheng-Nian Luo[a,*], J.G. Swadener[b], Chi Ma[c], Oliver Tschauner[d]

[a]Physics Division, Los Alamos National Laboratory, Los Alamos, NM 87545, USA
[b]Center for Integrated Nanotechnologies, Los Alamos National Laboratory, Los Alamos, NM 87545, USA
[c]Division of Geological and Planetary Sciences, California Institute of Technology, Pasadena, CA 91125, USA
[d]Department of Physics and High Pressure Science and Engineering Center, University of Nevada, Las Vegas, NV 89154, USA

Received 1 March 2007; received in revised form 30 May 2007; accepted 2 June 2007

Abstract

We conducted nanoindentation to explore the hardness and elastic properties of silica stishovite, synthesized at high pressure and quenched to ambient conditions. A total of 10 crystallographic orientations were examined on selected grains with a maximum load of 4 or 20 mN. We observed discontinuity in the load–displacement curve (pop-in) for the [2 5 $\bar{1}$] and [6 2 $\bar{1}$] grains subjected to a maximum load of 20 mN. The single-crystal hardness at high plastic deformation is quasi-isotropic with an average of 32 ± 1 GPa, similar to the polycrystalline hardness reported earlier; the theoretical hardness determined from the experiments is about 54 ± 3 GPa. These two hardnesses suggest that stishovite is one of the hardest oxides. The measured indentation moduli are close to the predictions at low load (minor plasticity) but are considerably lower at high load (high plasticity). Both indentation hardness and modulus decrease with increasing plasticity. Our results underscore the necessity of considering the degree of plastic deformation when interpreting hardness and elastic moduli from indentation experiments.

PACS: 62.20.−x; 62.20.Qp; 91.60.Dc

Keywords: Silica stishovite; Nanoindentation; Hardness; Elastic modulus

1. Introduction

Stishovite [1], a high-pressure polymorph of silica, is arguably one of the hardest oxides [2]. Its hardness was claimed to be secondary to the cotunnite-type TiO_2 synthesized at much higher a pressure of 60 GPa (compared to ~10 GPa for stishovite) [3]. Given its potential applications as a hard material and relative ease of synthesis, and implications to its plastic deformation in the Earth's interior, some experiments have been conducted to investigate its hardness and elastic properties [1–5]. However, an appreciable scatter in hardness measurements was observed, ranging from 21 to 33 GPa [1–3,5]. For tetragonal single-crystal stishovite, its hardness may be anisotropic; a recent work by Brazhkin et al. reported a hardness of 31.8 ± 1.0 GPa along the *c*-axis and of 26.2 ± 1.0 GPa along a perpendicular direction [5]. To draw a definitive conclusion on the hardness anisotropy of stishovite, it is necessary to examine systematically the hardness along various crystallographic orientations. Depending on the indentation load, discontinuity may occur in the load–displacement curve (i.e., the pop-in event [6,7] due to a discrete elastic–plastic deformation [8]). It has long been noted that a crystalline material demonstrates an extraordinarily high strength prior to the pop-in events, and then deforms approximately in an elasto-plastic manner with decreasing strength until certain maximum depth [8]. This phenomenon is referred to as the indentation size effect possibly associated with geometrically necessary dislocations [8–10]. Indentation elastic moduli also depend on the extent of deformation as different

*Corresponding author. Tel.: +1 505 664 0037; fax: +1 505 665 3552.
E-mail address: sluo@lanl.gov (S.-N. Luo).

0921-4526/$ - see front matter © 2007 Elsevier B.V. All rights reserved.
doi:10.1016/j.physb.2007.06.011

defects and plasticity are induced as deformation progresses [11]. However, the deformation dependence of the indentation elastic moduli and hardness has often been neglected, and has not been addressed for stishovite in particular. Here we have conducted nanoindentation at two representative maximum loads (one of which induced pop-in, and the other, did not), and investigated the orientation dependence of the hardness of single stishovite grains, and the deformation dependence of indentation hardness and elastic moduli.

2. Experiments

The stishovite specimen was synthesized from silica glass in a multi-anvil high-pressure press at nominal conditions of 14 GPa and 1273 K, using a Re foil heater/sample container, a sintered MgO octahedron, tungsten carbide anvils and pyrophyllite gaskets, then quenched to ambient conditions; the synthesis procedure was detailed elsewhere [12]. X-ray diffraction revealed only the tetragonal stishovite phase (space group $P4_2/mnm$) [13]. The specimen, about 2 mm across and 0.4 mm thick, was polished with diamond powder and colloidal silica suspension to sub-micron finish and to remove amorphous surface layer.

Polished sections of the specimen were coated with a thin carbon layer and examined with a LEO 1550VP field emission scanning electron microscope (SEM). Orientation analyses of single stishovite grains were preformed using an HKL electron back scatter diffraction (EBSD) system operated at 20 kV and 1 nA with a focused beam and a 70° tilted stage. The EBSD system was calibrated using a single-crystal silicon standard. The EBSD patterns were indexed for orienting individual grains. Shown in Fig. 1(a) are examples of SEM image and EBSD indexing. The grain size of the polycrystalline stishovite sample ranged from a few to 100's μm.

We selected a total of 10 grains for nanoindentation, considering both grain size and crystallographic orientation. The pole figures of 10 orientations of these selected stishovite grains are shown in Fig. 1(b), and these orientations were sufficiently representative. The indentation test was conducted with a Berkovich diamond nanoindenter, and sequentially consisted of loading at a rate of 0.3 mN/s to a maximum load (P_{max}) of 20 mN, holding at a constant load of 20 mN for 10 s, unloading at a rate of 0.3 mN/s to a load of 2 mN, holding at a constant load of 2 mN for 100 s, and unloading completely at a rate of 0.3 mN/s. During the 100 s hold period, the thermal drift rate was determined for each test, and a drift rate correction was applied to each test using this value. The measured drift rates were within the range ±0.06 nm/s. In addition, two grains were tested to a maximum load of 4 mN using the same protocol, except that the loading and unloading rates were 0.1 mN/s. A minimum of five nanoindentation tests, spaced a minimum of 10 μm apart, were conducted on each grain, and their results averaged. If space permitted on the grain, a sixth indentation was made. An example of the atomic force microscopy (AFM) image

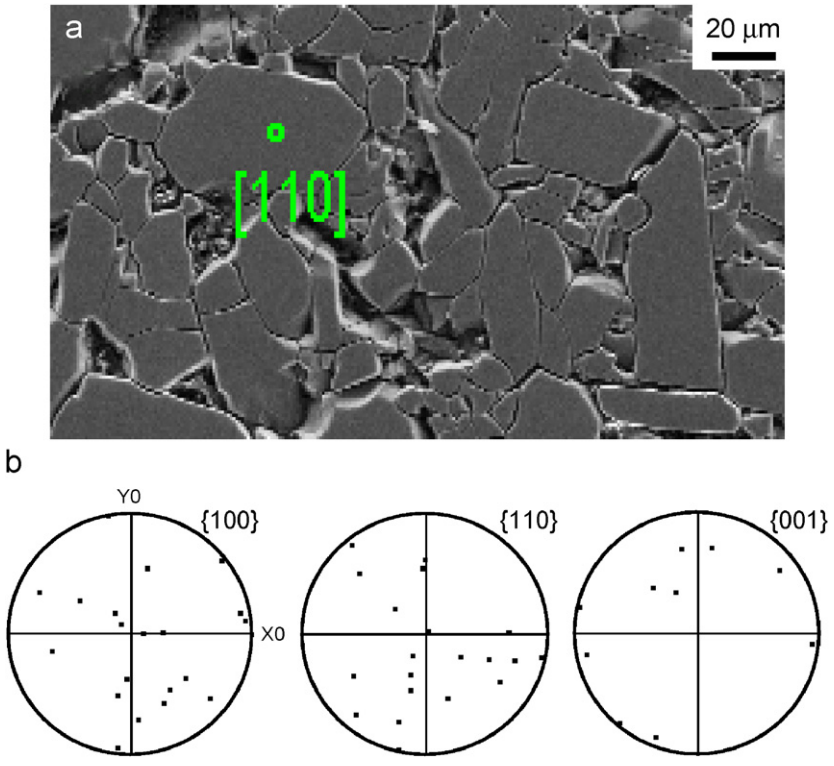

Fig. 1. (a) Representative SEM image of an area on the surface of the stishovite specimen, where the grain [1 1 0] was selected for nanoindentation; (b) pole figures of crystallographic orientations of ten selected stishovite grains constructed from equal area projection to the upper hemispheres.

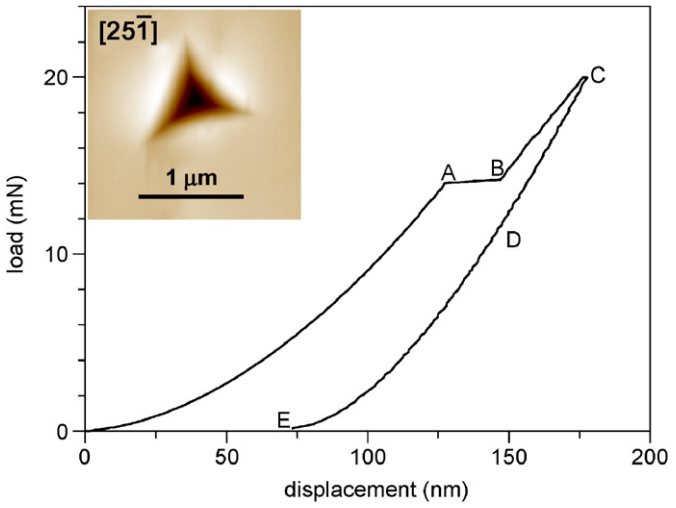

Fig. 2. Load–displacement curve for nanoindentation on the [2 5 $\bar{1}$] grain with a pop-in (*AB*) at about 14 mN. *Inset*: a two-dimensional AFM image of the indent.

of the indents is shown in Fig. 2 inset. The edge length of the indents in our experiments was below 1 μm for P_{max} of 20 mN, much smaller than the grain size (50–200 μm). Thus our results should be regarded as for single crystals. The area function of the indenter tip was calibrated using the Oliver–Pharr method [14]. Comparison with known standards gave an uncertainty of ±5% for the calibration.

3. Results and discussion

The load–displacement curves were obtained for selected grains with specific surface normals. No pop-in was observed except on the [2 5 $\bar{1}$] and [6 2 $\bar{1}$] grains for $P_{max} = 20$ mN; continuous plasticity deformation in current experimental time scales could have prevented us from observing pop-ins for other crystallographic planes. Typical indentation depth was 150–200 nm for $P_{max} = 20$ mN. An example of the load–displacement curve with a pop-in event is shown in Fig. 2 for the [2 5 $\bar{1}$] grain, and the onset of the pop-in is at about 14 mN and 125 nm. Further indentation tests were conducted on the [2 5 $\bar{1}$] and [6 2 $\bar{1}$] grains with $P_{max} = 4$ mN, and no pop-in was induced as expected.

A pop-in has normally been related to the onset of the elastic–plastic transitions, and the loading segment prior to the pop-in (e.g., *OA* in Fig. 2) is thus often regarded as purely elastic [8,15]. However, for the run of the [2 5 $\bar{1}$] grain with $P_{max} = 4$ mN, the strain did not recover completely after complete unloading: the deformation at the peak load was plastic by definition (the minor plasticity might be dislocations). Previous classification of the deformation prior to a pop-in as purely elastic appears over-generalized. We thus classified the deformation along a loading curve into three regimes: (I) perfectly elastic deformation, (II) small plastic deformation before pop-in and (III) relatively large plastic deformation after pop-in. The deformation at the peak load for the [2 5 $\bar{1}$] grain with $P_{max} = 4$ mN was in regime II, and regime I was below 4 mN for this run; there was no evident indication of the transition from regime I to II. The deformation at the peak load for all other runs with $P_{max} = 20$ mN was in regime III. Note that pop-in did not occur in every orientation. For some grain orientations, the large plastic deformation occurred gradually. So these three regimes may not be identified visually in a load–displacement curve.

We analyzed the upper half of the unloading portion of the load–displacement curve (e.g., *CD* in Fig. 2) following the Oliver–Pharr method [14] for deducing both hardness and elastic properties. The hardness is defined as $H \equiv P_{max}/A$, where A is the contact area. The indentation modulus is $M = (\sqrt{\pi}/2)(S/\sqrt{A})$, where S is the measured contact stiffness. (More details on the method can be found in Ref. [14].) The run-averaged results of M and H are shown in Table 1 for different grain orientations.

Presumably, the hardness measured on a specific crystallographic plane depends on the associated atomic packing, and may thus be anisotropic. Indeed, the pop-in behavior of stishovite is anisotropic, indicating a plastic anisotropy. However, with a maximum load of 20 mN, H for the two grains with apparent pop-ins ([2 5 $\bar{1}$] and [6 2 $\bar{1}$]) is nearly the same as other grains for which pop-ins were not recorded. H is quasi-isotropic with an average of 32 ± 1 GPa, in excellent agreement with the so-called polycrystalline hardness reported previously [2,3]. This weak anisotropy is in contrast with the pronounced elastic anisotropy [16] for stishovite; for example, its transverse anisotropy A_T is $C_{44}/C_{66} \approx 0.8$ for the (0 1 0) or (1 0 0) symmetry plane, and $2C_{44}/(C_{11} - C_{12}) \approx 2.1$ for the (1 $\bar{1}$ 0) plane. (The elastic moduli C_{ij} were obtained with a Brillouin scattering technique; $C_{11} = 453$, $C_{33} = 776$, $C_{44} = 252$, $C_{66} = 302$, $C_{12} = 211$, and $C_{13} = 203$ in units of GPa [4]. Similar results [5] were also obtained.) The elastic anisotropy of the pristine stishovite is also shown in Fig. 3 (the curves calculated from C_{ij} listed above). This observation suggests that at sufficient plastic deformation (e.g., regime III), the hardness of a single crystal becomes quasi-isotropic and approaches the average (polycrystalline

Table 1
Indentation modulus and hardness for individual stishovite grains, measured on surfaces with specific normals (**n**)

n	M (GPa)	H (GPa)	P_{max} (mN)	Pop-in
[6 2 $\bar{1}$]	411 (39)	31.3 (0.7)	20	Yes
[0 3 $\bar{5}$]	478 (50)	32.1 (0.8)	20	No
[0 4 $\bar{1}$]	390 (27)	30.2 (1.8)	20	No
[2 5 $\bar{1}$]	462 (14)	33.5 (0.6)	20	Yes
	500 (19)	54.0 (3.0)	4	No
[5 4 3]	396 (38)	31.4 (1.0)	20	No
[6 1 1]	353 (18)	31.4 (0.5)	20	No
[1 2 $\bar{6}$]	465 (58)	32.9 (1.2)	20	No
[1 6 $\bar{6}$]	494 (27)	32.5 (1.1)	20	No
[1 1 0]	449 (26)	31.8 (1.6)	20	No
[4 5 6]	449 (14)	31.5 (0.4)	20	No

Average values are given with standard deviations in parentheses.

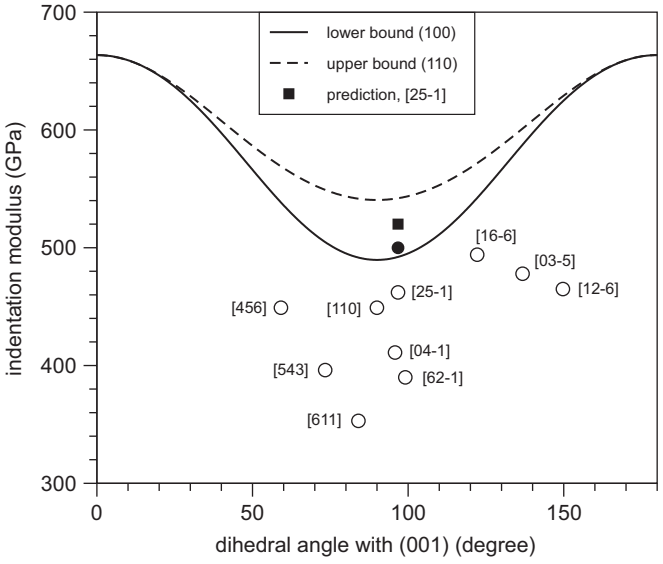

Fig. 3. Indentation modulus versus the dihedral angle between the indentation surface and (0 0 1). Curves and square are theoretical predictions: the upper and lower bounds refer to the indentation surfaces whose normals lie respectively in (1 1 0) and (1 0 0). Open circles denote experiments with $P_{max} = 20\,mN$, and the filled circle, $P_{max} = 4\,mN$ for [2 5 $\bar{1}$].

or conventional) hardness, despite its anisotropy in elasticity and early stage plasticity. Possibly, the plasticity saturated at a certain load is nearly isotropic. Compared to the polycrystalline hardness of about 38 GPa for the cotunnite-type TiO_2 claimed to be the hardest oxide [3], stishovite has a slightly lower value of 32 GPa; however, it is much easier to synthesize stishovite in bulk quantity than the cotunnite-type TiO_2 (about 10 GPa vs. 60 GPa).

Nonetheless, H is 54 ± 3 GPa on the [2 5 $\bar{1}$] grain for $P_{max} = 4\,mN$ without a pop-in, about 70% higher than the value obtained with $P_{max} = 20\,mN$ with a pop-in. (No conclusive result was obtained for [6 2 $\bar{1}$] due to pronounced scatter in measurements.) Appreciably higher strength has often been observed prior to pop-in, and the hardness prior to pop-in is a natural approximation to the theoretical hardness of the crystal itself [8,15,17]. As indicated by Martínez and Esteve in their experiments on tetrahedral amorphous diamond [18], the theoretical hardness should be measured at the maximum load in purely elastic regime, for instance, slightly below pop-in, *if* the deformation prior to the pop-in is purely elastic. However, minor plastic deformation (regime II) actually occurred on the [2 5 $\bar{1}$] grain for $P_{max} = 4\,mN$; thus, its elastic limit is below 4 and 14 mN near the pop-in (Fig. 2). We simply take H of 54 ± 3 GPa as a close approximation to the theoretical hardness of stishovite.

Besides the cotunnite-type TiO_2, sapphire (α-Al_2O_3) is another oxide rivaling stishovite in hardness. Deformation regimes I–III have been observed for sapphire single crystals [6,15]. The hardness of sapphire in plastic regime was reported as 19–21 GPa [2,3] and 36 ± 7 GPa [19], and the latter was obtained at $P_{max} = 5\,mN$ using a cube-corner diamond indenter. The difference might be due to the dependence of hardness on the extent of plastic deformation, or the samples used (single-crystal vs. polycrystalline). Thus, stishovite is at least comparable to sapphire in hardness. The "conventional" hardnesses of stishovite and sapphire appear to be secondary to the cotunnite-type TiO_2 (38 GPa); however, systematic work on the latter including single crystal hardness is necessary for a more meaningful comparison among them.

In anisotropic materials, indentation modulus M is a combination of all of the elastic constants weighted in favor of the normal direction, and can be predicted from known C_{ij} using the methodology presented elsewhere [20,21]. Conversely, C_{ij} can be calculated from various M on different crystallographic planes. The assumption for deducing C_{ij} of pristine single crystals from indentation is that the indented area is still in purely elastic regime I, and it has nonetheless often been neglected.

In regime I, the Hertz elastic model can be applied to deducing indentation modulus [22]. The deformation in all our runs reached regimes II and III (plastic), and the indentation moduli were thus deduced using the Oliver–Pharr method [14]. However, the indentation moduli deduced from regime III would be significantly lower than the predictions based on known C_{ij} for the pristine single-crystal stishovite, because of pronounced plasticity and defects. However, M deduced in regime II should be close to the prediction. The effect of plastic deformation on indentation modulus was explored below.

Based on independently measured C_{ij} as listed above [4], M was predicted as a function of crystallographic orientations for comparison with our independent measurements; both predicted and experimental values were plotted [21] as a function of the dihedral angle between the indentation surface and the (0 0 1) plane (Fig. 3). The M values obtained with a maximum load of 20 mN (regime III) are considerably lower than the predictions by about 50–150 GPa, and do not manifest the expected anisotropy, consistent with the weak anisotropy of the hardness. These values deduced from the indentation tests simply reflect the elastic properties of highly deformed but not the pristine stishovite. However, M of 500 ± 19 GPa, measured on the [2 5 $\bar{1}$] grain with P_{max} of 4 mN (no pop-in; regime II), is only slightly lower than the prediction (517 GPa) as expected (filled circle vs. square, Fig. 3); this high value of M is also consistent with the high value of H (roughly the theoretical strength). The much lower values of M (compared to the predictions) obtained for $P_{max} = 20\,mN$ can be readily attributed to the large plastic deformation and defects at this load, in contrast to the minor plasticity in the indented regime on the [2 5 $\bar{1}$] grain ($P_{max} = 4\,mN$).

The dependence of H and M on the extent of plastic deformation can also be seen from continuous stiffness measurements [14] during indentation (i.e., loading along a single load–displacement curve): M and H determined in this way were found to decrease during loading as the materials underwent progressive plastic deformation.

Similar observation on hardness has been made for sapphire in regimes II and III [15]. The weakening in mechanical properties happened gradually over a 50–100 nm indentation depth except the $[2\,5\,\bar{1}]$ and $[6\,2\,\bar{1}]$ grains, for which the decrease coincided with pop-in. Pop-in is often related to the onset of *pronounced* plasticity [8,14] and may thus depend on orientation: the kinetic energy barriers for nucleation and propagation of dislocation and twinning are anisotropic; pop-in was not observed for other grains due to their substantially different kinetics in our experimental time scales. Pop-in observed in sapphire was attributed to the formation of a twinned structure [6]. Twinning is also a possible explanation for the decrease of hardness and modulus observed in these experiments on stishovite. Dislocations may have formed during loading, but likely reversed partly upon unloading. The minor plasticity observed for the $[2\,5\,\bar{1}]$ grain at $P_{max} = 4$ mN (prior to pop-in) may be associated with dislocations. The results are not in agreement with a phase change to any known phase of SiO_2.

H and M both decrease with increasing plastic deformation, consistent with the indentation size effect previously generalized [8,9]; and it may account for the scatter found in previous experiments [1–3,5]. Thus, the extent of deformation (plasticity and defects like microcracks) should be considered when interpreting indentation measurements. The definition of hardness has been vague, making it difficult for a meaningful comparison among reported values [11]. An appropriate index of hardness can be the theoretical strength (approximately, the hardness prior to pop-in), or the indentation depth independent hardness in highly plastic regime [8]. Similarly, the elastic moduli deduced from indentation also depend on deformation, and are meaningful only at the elastic deformation regime in order to be used to deduce C_{ij} for the pristine crystals.

4. Conclusion

The indentation hardness and elastic modulus of stishovite have been investigated with nanoindentation for 10 crystallographic orientations, and found to decrease with increasing plastic deformation. For a maximum load of 20 mN, pop-in occurred on the $[2\,5\,\bar{1}]$ and $[6\,2\,\bar{1}]$ grains; the single-crystal hardness is quasi-isotropic and its average is 32 ± 1 GPa, similar to the polycrystalline hardness previously reported; the deduced indentation modulus for a specific orientation is significantly lower than prediction. For a maximum load of 4 mN, the hardness is 54 ± 3 GPa for the $[2\,5\,\bar{1}]$ grain and approximately the theoretical hardness, and its indentation modulus is close to prediction. Our results suggest that, a meaningful comparison of indentation hardness and modulus requires considering their deformation dependences.

Acknowledgments

We thank Drs. J.L. Mosenfelder and P.D. Asimow for their help with the sample synthesis, and R.N. Mulford for stimulating discussion. SEM and EBSD analyses were carried out at the Caltech GPS Division Analytical Facility which is supported in part by the MRSEC Program of the NSF under DMR-0080065. LANL is under the auspices of the U.S. Department of Energy.

References

[1] S.M. Stishov, S.V. Popova, Geochem. 10 (1961) 923.
[2] J.M. Leger, J. Haines, M. Schmidt, J.P. Petitet, A.S. Pereira, J.A.H. da Jornada, Nature 383 (1996) 401.
[3] L.S. Dubrovinsky, N.A. Dubrovinskaia, V. Swamy, J. Muscat, N.M. Harrison, R. Ahuja, B. Holm, B. Johansson, Nature 405 (2001) 653.
[4] D.J. Weidner, J.D. Bass, A.E. Ringwood, W. Sinclair, J. Geophys. Res. 87 (1982) 4740.
[5] V.V. Brazhkin, M. Grimsditch, I. Guedes, N.A. Bendeliani, T.I. Dyuzheva, L.M. Lityagina, Phys.-Usp. 45 (2002) 447.
[6] R. Nowak, T. Sekino, K. Niihara, Philos. Mag. A 74 (1996) 171.
[7] W.W. Gerberich, J.C. Nelson, E.T. Lilleodden, P. Anderson, J.T. Wyrobek, Acta Mater. 44 (1996) 3585.
[8] K. Durst, B. Backes, O. Franke, M. Göken, Acta Mater. 54 (2006) 2547.
[9] Q. Ma, D.R. Clarke, J. Mater. Res. 10 (1995) 853.
[10] M.F. Ashby, Philos. Mag. 21 (1970) 399.
[11] J. Malzbender, J. Eur. Ceram. Soc. 23 (2003) 1355.
[12] S.N. Luo, J.L. Mosenfelder, P.D. Asimow, T.J. Ahrens, Geophys. Res. Lett. 29 (2002) 1691.
[13] N.L. Ross, J.F. Shu, R.M. Hazen, T. Gasparik, Am. Mineral. 75 (1990) 739.
[14] W.C. Oliver, G.M. Pharr, J. Mater. Res. 7 (1992) 1564.
[15] T.F. Page, W.C. Oliver, C.J. McHargue, J. Mater. Res. 7 (1992) 450.
[16] K. Lau, A.K. McCurdy, Phys. Rev. B 58 (1998) 8980.
[17] N. Gane, F.P. Bowden, J. Appl. Phys. 39 (1968) 1432.
[18] E. Martínez, J. Esteve, Appl. Phys. A 72 (2001) 319.
[19] M.P. Shemkunas, W.T. Petuskey, A.V.G. Chizmeshya, K. Leinenweber, G.H. Wolf, J. Mater. Res. 19 (2004) 1392.
[20] J.J. Vlassak, W.D. Nix, Philos. Mag. A 67 (1993) 1045.
[21] J.G. Swadener, G.M. Pharr, Philos. Mag. A 81 (2001) 447.
[22] W. Wang, K. Lu, Philos. Mag. 86 (2006) 5309.